Effects of the density perturbation in scattering

Tae-Kyung Hong

Earth Sciences Department/Institute of Geophysics and Planetary Physics, University of California, Santa Cruz, California, USA

B. L. N. Kennett

Research School of Earth Sciences, Australian National University, Canberra, ACT, Australia

Ru-Shan Wu

Earth Sciences Department/Institute of Geophysics and Planetary Physics, University of California, Santa Cruz, California, USA

Received 9 March 2004; revised 3 May 2004; accepted 8 June 2004; published 1 July 2004.

[1] The influence of density variation on scattering is investigated in terms of attenuation, coda level, and apparent frequency shift. The influence of density variations is to produce more scattered energy than for velocity perturbations alone with a consequently higher coda level. The temporal decay of the coda is reduced, so that high perturbations in density are associated with a long duration of coda. These effects are particularly important for media with small-scale heterogeneity. Thus inversions for heterogeneity parameters, based on the character of precursors and coda of seismic phases penetrating deep into the Earth, need to take into account the nature of the density variations as well as wave speed variations. *INDEX TERMS:* 7203 Seismology: Body wave propagation; 7260 Seismology: Theory and modeling; 7299 Seismology: General or miscellaneous. **Citation:** Hong, T.-K., B. L. N. Kennett, and R.-S. Wu (2004), Effects of the density perturbation in scattering, *Geophys. Res. Lett.*, *31*, L13602, doi:10.1029/2004GL019933.

1. Introduction

[2] In the Earth, physical or chemical variation in materials causes changes in velocities and the density of media. As a result of the perturbation in physical parameters, scattered waves are generated. These scattered waves are recorded in a form of precursors and coda waves with time records, and they are widely used for the investigation of the properties of media. In particular, the precursors and coda waves of seismic deep phases (e.g., PKP, PcP) are useful particularly in the detection of small-scale heterogeneities [e.g., *Hedlin et al.*, 1997; *Vidale and Hedlin*, 1998; *Niu and Wen*, 2001].

[3] Since, however, scattering of seismic waves is the result of composite effect of perturbations in Lamé coefficients and the density, the resultant scattering effect varies with the combination of physical parameters. Thus, the interpretation of scattered waves in terms of both velocity and density perturbations may be desirable for correct inference of the physical state of medium, especially where high physical and chemical transition is present, such as, the partial-melting region at the core-mantle boundary [*Vidale and Hedlin*, 1998]. However, little attention has been paid to the density perturbation in analyses based on scattered waves, and its effect on scattering has scarcely been explored in the case of real data inversion.

[4] Numerical forward modelling is useful for the investigation of the effect of specific parameters, and has been applied for studies on scattering in the deep Earth [e.g., *Emery et al.*, 1999; *Furumura et al.*, 1999] and for the measurement of attenuation by scattering [e.g., *Roth and Korn*, 1993; *Frankel and Clayton*, 1986; *Hong and Kennett*, 2003a]. We investigate effects of density perturbation in terms of scattering attenuation and coda energy, and discuss the way to detect the density variation from seismic responses.

2. Wave Equation and Model

[5] In order to probe the pure effects by the density perturbation, we consider 2-D *SH* waves which are not affected by wave-type coupling and polarization. Acoustic (scalar) waves are implemented complementarily for the exploration of the influence of shear-modulus (Lamé coefficients) perturbation in scattering. Here, the 2-D *SH*-wave equation is given by

$$\frac{\partial^2 u}{\partial t^2} = \frac{1}{\rho}\frac{\partial}{\partial x}\left(\mu\frac{\partial u}{\partial x}\right) + \frac{1}{\rho}\frac{\partial}{\partial z}\left(\mu\frac{\partial u}{\partial z}\right), \tag{1}$$

where u is the displacement, c is the wave velocity, ρ is the density, and μ is the shear modulus. The velocity of *SH* waves is $\sqrt{\mu/\rho}$.

[6] Considering the structure of the Earth [*Kennett et al.*, 1995] and well-log results for small-scale heterogeneities in the Earth [*Shiomi et al.*, 1997], a physical or chemical property transition produces a change in both wave velocities and the density. Also, the quantities are expected to vary proportionally. Thus, the perturbations in wavespeeds and the density can be represented simply as [e.g., *Sato and Fehler*, 1998]

$$\xi(\mathbf{x}) = \frac{\delta c(\mathbf{x})}{c_0} = \frac{1}{K(\mathbf{x})}\frac{\delta\rho(\mathbf{x})}{\rho_0}, \tag{2}$$

where $\xi(\mathbf{x})$ is the velocity perturbation strength at location $\mathbf{x}$, the subscript 0 indicates the background quantities, δ represents the perturbation amount, and K is the parameter controlling the density perturbation relative to the velocity

0094-8276/04/2004GL019933$05.00

perturbation. It is difficult to constrain the density perturbation strength (K) from seismic observation [*Kennett*, 1998; *Romanowicz*, 2001]. The K varies with the location in the Earth and was reported to be $K = 0.2-0.3$ and $K > 0.6$ in the mid and lower mantle (*Romanowicz*, 2001).

[7] We consider von Karman random media with Hurst number (ν) of 0.25 [see *Hong and Kennett*, 2003a]. The size of the media is 57.6 km-by-115.2 km, which is represented by 256-by-512 grid points. Plane waves are incident vertically and 128 receivers with a uniform interval of 450 m are placed at a distance of 83.7 km. The wavespeed and the density in the background media are 7.2 km/s and 5.4 g/cm^3, which are plausible in the lower mantle [*Kennett et al.*, 1995]. The source time function of the incident waves is the Ricker wavelets with the dominant frequency of 4.5 Hz, and the wavelength is 1.6 km. Four scales of random heterogeneities (a = 249.5, 626.9, 1574.9, 3955.7 m, where a is the correlation length) are considered. Note that the corresponding normalized wavenumbers (ka) for the dominant frequency are 0.98, 2.46, 6.18 and 15.53. The perturbation in wavespeed varies from 1.7% to 9%, and four representative density perturbations (K = 0, 0.4, 0.8, 1.6) are considered for each velocity perturbation. A wavelet-based method (*Hong and Kennett*, 2002, 2003b), which retains high accuracy and stability even in strongly perturbed media, is implemented for modelling of wave propagation in random media.

3. Scattering Attenuation

[8] Theoretical scattering attenuation of 2-D acoustic and *SH* waves with density perturbation can be formulated based on a single scattering approximation [*Wu*, 1982; *Frankel and Clayton*, 1986] by

$$\frac{Q_s^{-1}}{\epsilon^2} = \frac{k^2}{4\pi} C_e \int_{\theta_{\min}}^{\pi} \mathcal{P}\left(2k \sin\frac{\theta}{2}\right) d\theta, \qquad (3)$$

where k is the wavenumber of incident waves and $\mathcal{P}$ is the power spectral density function of random heterogeneities. The magnitude of the constant C_e is 4 for acoustic waves, while it varies with the density perturbation in *SH* waves. The value of C_e in *SH* waves corresponds to the ensemble average of $[C_1 + C_2(1 - \cos\theta)]^2$ for random angle (θ) from 0 to 2π, where $C_1 = -2$ and $C_2 = K + 2$, and they are given by 2.0, 3.04, 4.56 and 9.04 for K = 0, 0.4, 0.8 and 1.6 respectively. Theoretically, scattering attenuation is expected to increase with the density perturbation (see Figure 1).

[9] From each numerical modelling, scattering attenuations are measured in a frequency range of 2–10 Hz using the stacked spectral seismogram. Here in order to exclude the influence of scattered waves from the stacked spectral responses, we initially filter off the scattered wavefield around primary waves from each time response by tapering with an adaptive time window (cosine bell) before the stacking in Fourier domain [*Hong and Kennett*, 2003a].

[10] The normalized scattering attenuations (Q_s^{-1}/ε^2) are determined to be very close for various velocity perturbations at media with small-scale heterogeneities (a = 249.5 m, $ka < 2$). However, at $ka > 2$ (e.g., a = 1574.9, 3955.7 m) the normalized scattering attenuation by high velocity perturbation is determined to be smaller than that by low velocity perturbation, and the difference increases with ka. The phenomenon may be related with the development of coherent forward scattered energy which increases with the perturbation strength. The feature is consistent regardless a change in density perturbation. Thus, the minimum scattering angle for the correction of forward scattering energy in equation (3) is determined as around 60°–90° at $ka < 2$, while it varies from 20° to 90° with perturbation strength in the range of $ka > 2$.

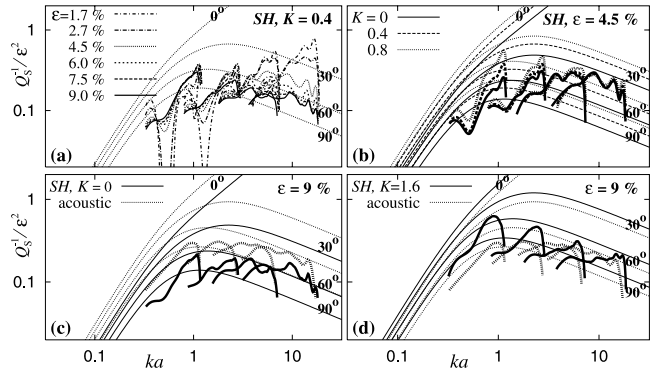

Figure 1. The variation of *SH* scattering attenuation (a) with velocity perturbations (ε = 1.7, 2.7, 4.5, 6.0, 7.5, 9.0%) for a constant density perturbation (K = 0.4), and (b) with density perturbation for a constant velocity perturbation (ϵ = 4.5%). Comparisons of scattering attenuation strengths between acoustic and SH ((c) K = 0, (d) K = 1.6) waves are presented. Theoretical scattering attenuation curves from equation (3) are embedded in the Figures. The scattering attenuation (Q_s^{-1}/ϵ^2) is determined close at low normalized wavenumber ($ka < 2$), but a large difference with change of velocity perturbation at large ka ($ka > 2$). Scattering attenuation is strengthened with density perturbation, particularly at $ka < 2$. *SH* waves display a lower scattering attenuation than acoustic waves at the low density perturbation (K = 0.4), but the introduction of a high density perturbation generates comparable or even higher scattering. Note that the patterns in (a) and (b) are observed in cases with different density perturbations.

[11] The increase of density perturbation strengthens the scattering in media of given velocity perturbation strengths. The scattering magnitude difference caused by density perturbation decreases gradually with ka, and becomes unnoticeable at $ka \gg 2$ (Figure 1b). The consideration of density perturbation at media with given velocity perturbation amplifies the strength of shear-modulus perturbation, which causes a large and frequent variation of shear modulus in media with small-scale heterogeneities. Mathematically, this makes the spatial differentiation of shear modulus (e.g., $\partial_x(\mu\partial_x u)$) amplified. On the other hand, the amplification of shear-modulus perturbation is relatively less effective in media with large-scale heterogeneities, which have a perturbation structure of spatially gradual transitions.

[12] The *SH* waves with mild density perturbations (K = 0, 0.4) display lower scattering attenuation levels relative to acoustic waves (Figure 1c). However, when the density perturbation is stronger than the velocity perturbation (e.g.,

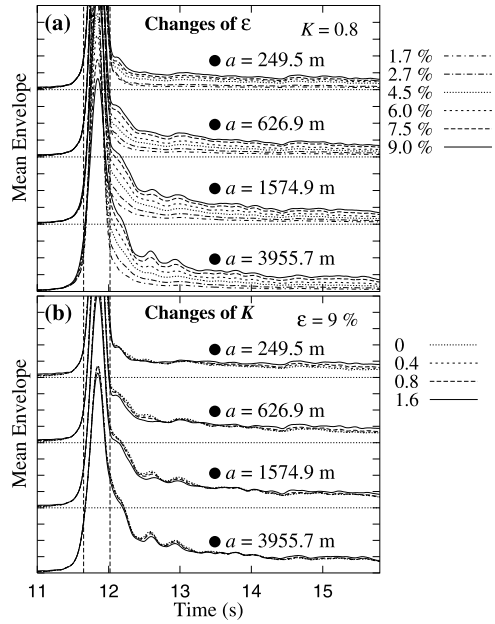

Figure 2. Mean envelopes of 128 time responses (a) for changes of velocity perturbations (ε = 1.7, 2.7, 4.5, 6.0, 7.5, 9.0%) and (b) density perturbations (K = 0, 0.4, 0.8, 1.6). The vertical dotted lines indicate the portion of the primary wave in homogeneous medium. The y-axis tick interval corresponds to 0.05 times of the incident-wave amplitude. The coda level increases with both velocity and density perturbation strengths. The coda level change with velocity perturbation is established from the beginning portion of coda waves, while that with density perturbation appears in a time lapse and is obvious in media with small-scale heterogeneities (a = 249.5 m). Density perturbation generates a less decaying coda waves.

K = 1.6, Figure 1d), the *SH* scattering attenuation is dominant over the acoustic scattering attenuation in the range of $ka < 2$. This energy attenuation with frequency is dependent on the wave-type and the density perturbation strength. In particular, in models with a constant velocity perturbation and a small scale of heterogeneity (e.g., a = 249.5, 626.9 m), the effect is stronger in the high frequency portion ($f > f_d$, where f_d is the dominant frequency) of transmitted waves (Figure 1b).

4. Stochastic Features

[13] With increase of velocity perturbation strength, both amplitude and phase fluctuations of primary waves grow. On the other hand, the density perturbation modulates mostly the amplitudes of time responses, but the phase fluctuation is scarcely affected when the velocity perturbation is kept constant.

[14] In order to measure scattered energy, envelope analysis has been widely adopted [e.g., *Hedlin et al.*, 1997]. In general, the level of coda waves is proportional to velocity perturbation strength (ε), and this fact is the theoretical basis of using envelope analysis for determination of perturbation strength from seismic data by comparing with theoretical prediction based on stochastic random models. Perturbation in the density, however, is another factor causing a change in scattering of seismic waves. In particular, the scattering by a high density perturbation ($K > 1$) looks to be large enough to mask the effect by velocity perturbation.

[15] From the envelope analysis results in Figure 2, several distinguishing features are observed. Firstly, the temporal decay rate of coda energy is nearly invariant with the change of velocity perturbations, but is reduced with increase of density perturbation. The coda level differences caused by the velocity perturbation change develop clearly even at the very beginning portion of coda waves. On the other hand, the coda level differences due to the change of the density perturbation appear in a time lapse after primary waves, and the gap between coda levels increases with time because of the difference in temporal decay rates. The relative variation of coda level with density perturbation is noticeable at small ka system (a = 249.5 m, ka = 0.98), but is negligibly small at large ka system (a = 3955.7 m, ka = 15.53). The coda level change introduced by the density perturbation is particulary remarkable at small ka system (ka = 0.98); the coda level with K = 1.6 is about twice of that with K = 0 at a time of 130% primary-wave travel, and it appears that the consideration of density factor looks crucial in field analysis based on coda waves.

[16] Another apparent phenomenon observed in waves transmitted through random media is the shift of the dominant frequency of primary waves to a lower frequency (Figure 3). Here, the dominant frequency of waves is measured from the stacked spectral seismograms which are used for the estimation of scattering attenuation. The apparent frequency shift is roughly proportional to the perturbation strength. The shift rate depends on the incident

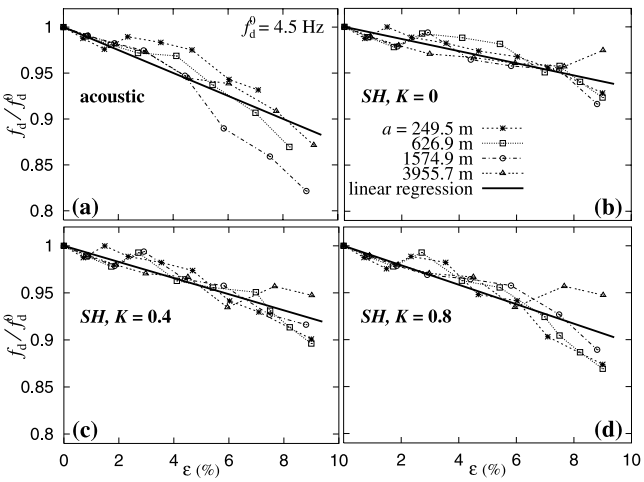

Figure 3. Apparent dominant frequency decrease of transmitted primary waves with perturbations: (a) acoustic waves and (b) *SH* waves with K = 0, (c) 0.4 and (d) 0.8. The average decrease rate of acoustic waves is 1.24, and those for *SH* waves with K = 0, 0.4 and 0.8 are 0.65, 0.85 and 1.03 respectively. The apparent frequency shift increases with density perturbation. The energy around the dominant and higher frequencies is attenuated dominantly during scattering, while the low-frequency energy is relatively less affected. The frequency shift rate appears to change steeper across around 5% perturbation, which may be a result of multiscattering dominance at high perturbation.

wave type, but is increased by the introduction of density perturbation (see, the solid lines in Figure 3). The decreasing rate may be divided into two regimes; the frequency-shift rate at high perturbation regime ($\varepsilon > 5\%$) is higher than the average rate, and it appears that multiscattering effect increases drastically with the perturbation strength.

5. Discussion and Conclusions

[17] Perturbation in the density plays a considerable role in the scattering of waves in random media. The density perturbation introduces additional scattering attenuation and raises the coda level. The effect is particular strong at low *ka* regime ($ka < 2$), but is weakened with *ka*. This scale (*ka*) dependency of density influence may be a promising feature for the sounding of fine-scale heterogeneities in the Earth's deep interior since low-frequency waves respond exclusively to a small-scale density variation in a high velocity region. As the frequency content of scattered waves is related with that of incident waves, velocity perturbation strength and heterogeneity scale can be determined with high-frequency band seismic data and the density perturbation can be constrained using low-frequency band data.

[18] The seismic phases transmitted from the deep Earth, such as *PKP* and P_{diff}, belong to such a category, and so an inverse study based on their precursors and coda waves is required to consider the effects of both velocity and density perturbation. Since the deep phases are expected to be rarely affected by the density perturbation in shallow structures due to the decrease of wavespeed, it looks possible to constrain the density variation in the Earth's deep interior, especially the partial-melting region at the core-mantle boundary [*Vidale and Hedlin*, 1998] where large density variation is expected. Moreover, since density perturbation amplifies in-phase scattered energy in the direction of P incidence, this consideration looks important for analysis of deep P phases. The generation of large long lasting coda by high density perturbation may be an explanation for the coda waves following Earth's deep reflection phases (e.g., *PKiKP*) which are observed to have very long duration.

[19] **Acknowledgments.** We are grateful to anonymous reviewers for the fruitful comments which improved the presentation of the paper. We acknowledge the Australian National University Supercomputer Facility for allocation of computational time in the Alpha server.

References

Emery, V., V. Maupin, and H.-C. Nataf (1999), Scattering of S waves diffracted at the core-mantle boundary: Forward modelling, *Geophys. J. Int.*, *139*, 325–344.

Frankel, A., and R. Clayton (1986), Finite difference simulation of seismic scattering: Implications for the propagation of short-period seismic waves in the crust and models in crustal heterogeneity, *J. Geophys. Res.*, *91*, 6465–6489.

Furumura, M., B. L. N. Kennett, and T. Furumura (1999), Seismic wavefield calculation for laterally heterogeneous Earth models II: The effect of upper mantle heterogeneity, *Geophys. J. Int.*, *138*, 623–644.

Hedlin, M. A., P. M. Shearer, and P. S. Earle (1997), Seismic evidence for small-scale heterogeneity throughout the Earth's mantle, *Nature*, *387*, 145–150.

Hong, T.-K., and B. L. N. Kennett (2002), On a wavelet-based method for the numerical simulation of wave propagation, *J. Comput. Phys.*, *183*, 577–622.

Hong, T.-K., and B. L. N. Kennett (2003a), Scattering attenuation of 2-D elastic waves: Theory and numerical modelling using a wavelet-based method, *Bull. Seismol. Soc. Am.*, *93*, 922–938.

Hong, T.-K., and B. L. N. Kennett (2003b), Modelling of seismic waves in heterogeneous media using a wavelet-based method: Application to fault and subduction zones, *Geophys. J. Int.*, *154*, 483–498.

Kennett, B. L. N. (1998), On the denisty distribution within the Earth, *Geophys. J. Int.*, *132*, 374–382.

Kennett, B. L. N., E. R. Engdahl, and R. Buland (1995), Constraints on seismic velocities in the Earth from travel times, *Geophys. J. Int.*, *122*, 108–124.

Niu, F., and L. Wen (2001), Strong seismic scatterers near the core-mantle boundary west of Mexico, *Geophys. Res. Lett.*, *28*, 3557–3560.

Romanowicz, B. (2001), Can we resolve 3D density heterogeneity in the lower mantle?, *Geophys. Res. Lett.*, *28*, 1107–1110.

Roth, M., and M. Korn (1993), Single scattering theory versus numerical modelling in 2-D random media, *Geophys. J. Int.*, *112*, 124–140.

Sato, H., and M. Fehler (1998), *Seismic Wave Propagation and Scattering in the Heterogeneous Earth*, Springer-Verlag, New York.

Shiomi, K., H. Sato, and M. Ohtake (1997), Broad-band power-law spectra of well-log data in Japan, *Geophys. J. Int.*, *130*, 57–64.

Vidale, J. E., and M. A. H. Hedlin (1998), Evidence for partial melt at the core–mantle boundary north of Tonga from the strong scattering of seismic waves, *Nature*, *391*, 682–685.

Wu, R.-S. (1982), Attenuation of short period seismic waves due to scattering, *Geophys. Res. Lett.*, *9*, 9–12.

T.-K. Hong and R.-S. Wu, Earth Sciences Department/IGPP, University of California, 1156 High Street, Santa Cruz, CA 95064, USA. (tkhong@es.ucsc.edu)

B. L. N. Kennett, Research School of Earth Sciences, Australian National University, Canberra, ACT, Australia.